A physics-based flexural phonon-dependent thermal conductivity model for single layer graphene

2013 Semicond. Sci. Technol. 28 015009

(http://iopscience.iop.org/0268-1242/28/1/015009)

Semicond. Sci. Technol. **28** (2013) 015009 (6pp) doi:10.1088/0268-1242/28/1/015009

A physics-based flexural phonon-dependent thermal conductivity model for single layer graphene

Rekha Verma, Sitangshu Bhattacharya and Santanu Mahapatra

Nano Scale Device Research Laboratory, Department of Electronic Systems Engineering, Indian Institute of Science, Bangalore 560012, India

E-mail: rekha.verma26@gmail.com, isbsin@yahoo.co.in and santanu@cedt.iisc.ernet.in

Received 5 June 2012, in final form 27 August 2012
Published 30 November 2012
Online at stacks.iop.org/SST/28/015009

Abstract

In this paper, we address a physics-based closed-form analytical model of flexural phonon-dependent diffusive thermal conductivity (κ) of suspended rectangular single layer graphene sheet. A quadratic dependence of the out-of-plane phonon frequency, generally called flexural phonons, on the phonon wave vector has been taken into account to analyze the behavior of κ at lower temperatures. Such a dependence has further been used for the determination of second-order three-phonon Umklapp and isotopic scatterings. We find that these behaviors in our model are best explained through the upper limit of Debye cut-off frequency in the second-order three-phonon Umklapp scattering of the long phonon waves that actually remove the thermal conductivity singularity by contributing a constant scattering rate at low frequencies and note that the out-of-plane Gruneisen parameter for these modes need not be too high. Using this, we clearly demonstrate that κ follows a $T^{1.5}$ and T^{-2} law at lower and higher temperatures in the absence of isotopes, respectively. However in their presence, the behavior of κ sharply deviates from the T^{-2} law at higher temperatures. The present geometry-dependent model of κ is found to possess an excellent match with various experimental data over a wide range of temperatures which can be put forward for efficient electro-thermal analyses of encased/supported graphene.

(Some figures may appear in colour only in the online journal)

1. Introduction

Graphene has emerged as a potential candidate for the next generation interconnects [1] and heat spreaders in integrated circuits (ICs) through its reportedly high thermal conductivity (κ) over conventional copper and aluminum [2]. In recent years, there have been a number of experiments on determining κ of single and multi-layers of both suspended [3–7] and on-substrate/encased graphene sheets and ribbons [8–11] over a wide range of temperatures. The outcome of these investigations was reported at room temperature thermal conductivity ranging from 2000 to 7000 W m^{-1} K^{-1} for suspended and about 600 W m^{-1} K^{-1} for on-substrate/encased single layer graphene (SLG) [2].

Presently, the realization of such a high thermal conductivity follows from the following active groups. According to Balandin's group [2–4, 11–15], the main contribution to the graphene κ comes from the in-plane longitudinal acoustic (LA) and transverse acoustic (TA) phonons, which are characterized by the high phonon group velocities and small Gruneisen parameters leading to the large phonon mean free path (MFP) [2]. Such an analysis follows from their full in-plane *ab initio*-based phonon dispersion relation for both these phonon modes which have been further evaluated through a number of simulative works using rigorous molecular dynamics approach, such as the use of the valance-force-field method [11, 16–18] for the determination of the exact phonon group velocities and Umklapp scattering selection rules. It is also stated that the contribution to the thermal conductivity from the out-of-plane phonon modes is small because of the large Gruneisen parameter and small group velocity. However, conversely Mariani and von Oppen

[19] used the rotational and reflection symmetries on the out-of-plane phonon branch, generally called flexural phonons, and later Lindsay *et al* [20, 21] used a nonlinear iterative approach to directly solve the linearized phonon Boltzmann's transport equation and predicted that the main contribution to both the suspended and on-substrate graphene κ comes from the large density of modes of the acoustic flexural phonon branch (ZA) whose dispersion relation is treated as nonlinear or rather quadratic in nature. This makes κ to follow a $T^{1.5}$ law variation below room temperature, also exhibited experimentally elsewhere [7, 22, 23]. However, there is an obvious inconsistency between the works of Xu *et al* [22] and Munoz *et al* [23]. It should be noted that the results by Xu *et al* [22] are most likely due to the low-quality graphene, which resulted in the low value of κ and specific $T^{1.5}$ temperature dependence. It has been long known for graphite that grain boundary and point defect scattering result in such dependences. The experimental works by Munoz *et al* [23] as the explanation of $T^{1.5}$ dependence deal specifically with the ballistic phonon transport regime, whereas Xu *et al* [22] specifically indicated that they deal with the diffusive transport regime. The latter was emphasized at the recent PHONONS 2012 conference [24]. Recently, Ong and Pop [25] used the reactive empirical bond order potential to consider C–C bonds for transport in graphene and Lennard-Jones potential for C–Si and C–O bonds to present the couplings with the surroundings for the determination of the heat flow mechanism and suggested that the inclusion of these modes is inevitable in order to explain the thermal conductivity of suspended as well as supported SLG, where these ZA modes are usually damped due to leakage through the substrate.

Hence we see from the above facts that it is still not clear about the role of the ZA phonon modes in order to explain the graphene thermal conductivity. Thus, to visualize their effect properly, at least for the preliminary step for the modeling approach, one should take into account the ZA phonon nonlinear dispersion relation for the evaluation of these phonon group velocities and thus its incorporation in Umklapp, and edge-roughness scatterings. The motivation of this study lies in the fact that although there have been few aforementioned developments on realizing the effect of the ZA phonons on graphene κ through various simulative and experimental works, however there is a deficiency in providing a physics-based closed-form analytical model for ZA phonon-dependent κ. This typical physics-based closed-form model is extremely needed in order to estimate the electro-thermal performances of these carbon-based materials through CAD tools, and to assess their reliability when fabricated as on-substrate or encased interconnects in future ICs [26, 27].

In what follows, we provide a closed-form thermal conductivity model to estimate the effect of the quadratic ZA phonon dispersion law on κ by determining the exact ZA phonon group velocities and use a second-order three-phonon Umklapp and edge-roughness scatterings and show that beyond room temperature κ of a pure flake follows a T^{-2} law due to the Umklapp scattering. However, below room temperature, we clearly demonstrate that the trend tends to experimentally established $T^{1.5}$ behavior. We find that these behaviors in our model are best explained through the upper limit of Debye cut-off frequency in the Umklapp scattering. We also find that the out-of-plane Gruneisen parameter for the ZA phonon dominated thermal conductivity need not be too high in predicting the magnitude of κ. In addition, we use the isotope scattering due to the addition of ^{13}C atom isotope on pure ^{12}C atom [15] which should be taken into account to model the commonly encountered situation where the difference in the atomic mass of carbon atoms is introduced unintentionally at the ends of the SLG under prevailing fabrication methods [28]. The introduction of the isotopes makes the SLG an impure one and marks wide variation in κ. Our present geometry-dependent closed-form analytical model of κ of SLG is in excellent match with the available experimental data over a wide range of temperatures and can be put forward to model efficient electro-thermal analyses for graphene-based interconnects.

2. Model development of thermal conductivity model for suspended SLG

The ZA phonon mode dominated diffusive thermal conductivity of an SLG sheet can mathematically be written as [7]

$$\kappa = \frac{1}{4\pi\delta k_B T^2}\int_{q=0}^{q_{\max}} \left(\frac{\partial\omega_q}{\partial q}\right)^2 (\hbar\omega_q)^2 \tau_q \frac{q\,\mathrm{e}^{\frac{\hbar\omega_q}{k_B T}}}{\left(\mathrm{e}^{\frac{\hbar\omega_q}{k_B T}}-1\right)^2}\,\mathrm{d}q \quad (1)$$

in which δ (=0.335 nm) is the layer thickness of an SLG [20], and $\partial\omega_q/\partial q$ is the ZA phonon velocity, where q is the ZA phonon vector, τ_p is the phonon scattering time and $\hbar$, k_B are the reduced Planck's constant and Boltzmann's constant, respectively. To obtain the out-of-plane phonon velocity, we use Landau's approach of Lagrangian for the long wavelength elastic distortion as [19, 29–31]

$$\mathcal{L} = \frac{\rho_0}{2}\left(\dot{\mathbf{u}}^2 + \dot{h}^2\right) - \frac{1}{2}\kappa_0\left(\nabla^2 h\right)^2 - \mu u_{ij}^2 - \frac{1}{2}\lambda u_{kk}^2 \quad (2)$$

in which $h(r)$ and $u(r)$ are the out-of-plane and in-plane distortions with the strain tensor $u_{ij} = \frac{1}{2}[\partial_i u_j + \partial_j u_i + (\partial_i h)(\partial_j h)]$. The parameters λ and μ are the Lame coefficients ($\mu \sim 3\lambda \sim 0.09$ eV nm^{-2}) and κ_0 (~ 1 eV) and ρ_0 (=7.6 $\times$ 10^{-7} Kg m^{-2}) are the bending rigidity and mass density, respectively, for graphene [30]. Using this, the flexural phonon dispersion relation can be written as [19, 30]

$$\omega_q = \alpha q^2 \quad (3)$$

in which $\alpha = \sqrt{\frac{\kappa_0}{\rho_0}} \approx 4.6\times10^{-7}$ m^2 s^{-1} denotes the ZA phonon diffusion constant. The use of equation (3) into equation (1) leads to the expression of κ as

$$\kappa = \frac{k_B^3 T^2}{2\pi\delta\hbar^2}\int_0^{\xi_{\max}} \tau_p \frac{\xi^3\,\mathrm{e}^{\xi}}{\left(\mathrm{e}^{\xi}-1\right)^2}\,\mathrm{d}\xi \quad (4)$$

in which $\xi = \frac{\hbar\omega_q}{k_B T}$ and $\xi_{\max} = \frac{\theta_D}{T}$, where θ_D is the Debye temperature ($\sim$1000 K [32]). In order to evaluate equation (4), we take the effect of edge-roughness scattering and second-order three-phonon scattering, whose relaxation rates can be written, respectively, for crystalline boundaries as [33, 34]

$$\frac{1}{\tau_E} = \frac{\sqrt{\pi}}{2F\sqrt{LW}}\left(\frac{\partial\omega_q}{\partial q}\right) \quad (5)$$

as the frequency-dependent edge-roughness scattering rate and

$$\frac{1}{\tau_U} = \frac{32}{27}|\gamma_{ZA}|^4 \left(\frac{k_B T}{M(\partial\omega_q/\partial q)^2}\right)^2 \omega_B \tag{6}$$

as the frequency-dependent second-order three-phonon scattering rate where F is the geometric factor, L and W are the length and width of the suspended SLG, M is the mass of the carbon atom, ω_B is the ZA phonon branch frequency and $|\gamma_{ZA}|$ is the Gruneisen parameter for the ZA mode. To capture the physical picture for why one should consider the second-order three-phonon anharmonic scattering process can be understood from Ziman's problem of long waves [35] which states that the thermal conductivity would keep increasing with the sample's size even if the low-frequency phonon MFP is limited by boundary scattering. Queries thus raised over whether the thermal conductivity of these materials would saturate with the increase in the length at or above room temperature were further considered using the phonon Umklapp process to the second order, which deals with the TA, ZA and LA mode contributions [36, 37]. It rather appeared that instead, if the first-order three-phonon processes (three-phonon process that of a virtual combination of two phonons of frequencies ω and ω' into an intermediate one, ω_i, and the splitting of that virtual phonon into two new phonons with frequencies ω'' and ω''') are considered for these materials, the thermal conductivity diverges with dimensions, the rate of variation being dependent on whether the phonon branches are linear or quadratic. It is rather the second-order three-phonon processes that actually remove this singularity by contributing a constant scattering rate at low frequencies [34]. Besides, the governing three-phonon scattering selection rules for SLG are as follows: exclusion of all three-phonon process having an odd number (1 or 3) of flexural phonons (for example, the following processes cannot occur: ZA+ZA↔ZA, ZA+TA↔TA, ZA+TA↔LA, ZA+LA↔LA, ZA+ZA↔ZO and ZA+ZO↔ZO, while ZA+ZA↔TA, LA and TA, LA↔ZA+ZA are allowed to occur) which stand valid for all the orders in SLG [20]. In addition to these scatterings, we also include the isotope-induced scattering where the linear dimensions of the defects are much smaller than the phonon wavelength. The effect of this isotope-induced scattering on κ of suspended SLG has recently been carried out through experiment and simulation as [15, 11]

$$\frac{1}{\tau_I} = \frac{1}{4} S_0 \Gamma_m \frac{q\omega_q^2}{(\partial\omega_q/\partial q)} \tag{7}$$

in which S_0 is the cross-sectional area per one atom ($= \delta \times r_0$), where $r_0 = 0.14$ nm is the carbon–carbon distance and the strength of the impurity scattering (Γ_m) can be defined as [15]

$$\Gamma_m = \sum_i f_i \left[\left(1 - \frac{M_i}{\overline{M}}\right)^2 + \varepsilon\left\{|\gamma_{ZA}|\left(1 - \frac{R_i}{\overline{R}}\right)\right\}^2\right], \tag{8}$$

where f_i is the fractional concentration of the impurity atoms, M_i and R_i are the mass and Pauling ionic radius of the ith impurity atom and $\overline{M}$ and $\overline{R}$ are the average atomic mass and radius with ε as a phenomenological parameter. It should be noted that the determination of the specific values of Γ_m is an extremely challenging work since the isotopic and average mass can be evaluated while the local displacement $(\overline{R}-R_i)$ as a result of the change of atom radius or bond length is usually unspecified [15]. However, rather to evaluate ε and $(\overline{R}-R_i)$, the order of Γ_m can be estimated from the knowledge of experimental data (as will be discussed later) and is generally found to be in the range of 10^{-6}–10^{-3} for low level to high level of isotope addition [38] for most materials. Furthermore, for the present case, we have taken the value of ZA phonon branch frequency ω_B to be 28 GHz which is less than that of two, three and four layers of graphene, respectively [39]. Thus following Matthiessen's rule, τ_p in equation (4) can be written using equations (5)–(7) as

$$\frac{1}{\tau_p} = \frac{1}{\tau_E} + \frac{1}{\tau_U} + \frac{1}{\tau_I}. \tag{9}$$

Using equation (3) equation (9) can further be simplified as

$$\frac{1}{\tau_p} = A\xi^{1/2} + \frac{B}{\xi^2} + C\xi^2 \tag{10}$$

in which $A = \frac{1}{F}\left(\frac{\pi\alpha k_B T}{\hbar LW}\right)^{1/2}$, $B = \frac{2}{27}\left(\frac{|\gamma_{ZA}|^4\hbar^2\omega_B}{M^2\alpha^2}\right)$ and $C = \frac{S_0\Gamma_m}{8\alpha}\left(\frac{k_B T}{\hbar}\right)^2$. From equation (10), it appears that the effect of edge-roughness scattering on κ of suspended SLG mainly dominates at the lower temperature in the absence of isotopes. This can be understood from the following: in the absence of isotopic impurity, the two scattering rates, i.e. edge-roughness and second-order three-phonon Umklapp scatterings are main. It can be seen from equation (10) that as temperature decreases, the Umklapp scattering rate goes down to zero leaving only the edge-roughness scattering to modulate the thermal conductivity. This leads to the expression of κ at lower temperature (κ_{low}) in pure SLG as

$$\kappa_{low} = \left(\frac{Fk_B}{2\delta}\right)\left(\frac{LW}{\alpha}\right)^{\frac{1}{2}}\left(\frac{k_B T}{\pi\hbar}\right)^{\frac{3}{2}}\left[\int_0^{\frac{\theta}{T}} \frac{\xi^{\frac{5}{2}}e^{\xi}}{(e^{\xi}-1)^2}d\xi\right]. \tag{11}$$

The last factor in the parenthesis is generally known as the Debye integral of order 5/2. It can be shown that in the lower temperature regime where the upper integral limit tends to infinity, this 5/2-order Debye integral converges to a numerical constant value 4.58. However, at the higher temperature regime, equation (4) converges to

$$\kappa_{high} = \left(\frac{k_B^3}{2\pi\delta}\right)\left(\frac{T}{\hbar}\right)^2\left[\int_0^{\frac{\theta}{T}}\left(\frac{\xi^3}{B+C\xi^4}\right)\frac{\xi^2 e^{\xi}}{(e^{\xi}-1)^2}\,d\xi\right], \tag{12}$$

which can finally be written as

$$\kappa_{high} = \left(\frac{k_B^3}{2\pi\delta}\right)\left(\frac{T}{\hbar}\right)^2\left(\frac{1}{4C}\right)\ln\left|1 + \frac{C}{B}\left(\frac{\theta}{T}\right)^2\right|. \tag{13}$$

In the absence of isotope density, equation (13) converges to

$$\kappa_{high} = \left(\frac{27}{16\pi\delta}\right)\left(\frac{k_B}{\hbar}\right)^3\left(\frac{M\alpha}{|\gamma_{ZA}|^2}\right)^2\left(\frac{\theta^4}{\hbar\omega_B}\right)\left(\frac{1}{T^2}\right), \tag{14}$$

whereas in the presence of heavy isotope concentration, equation (13) approaches

$$\kappa_{high} = \left(\frac{k_B\alpha}{\pi\delta S_0\Gamma_m}\right)\ln\left|\zeta\frac{\theta^4}{T^2}\right| \tag{15}$$

in which $\zeta = \left(\frac{27S_0\Gamma_m\alpha}{16\omega_B}\right)\left(\frac{k_B M}{\hbar^2|\gamma_{ZA}|^2}\right)^2$. While deriving equations (13)–(15), we have assumed that the function $\xi^2 e^{\xi}/(e^{\xi}-1)^2$

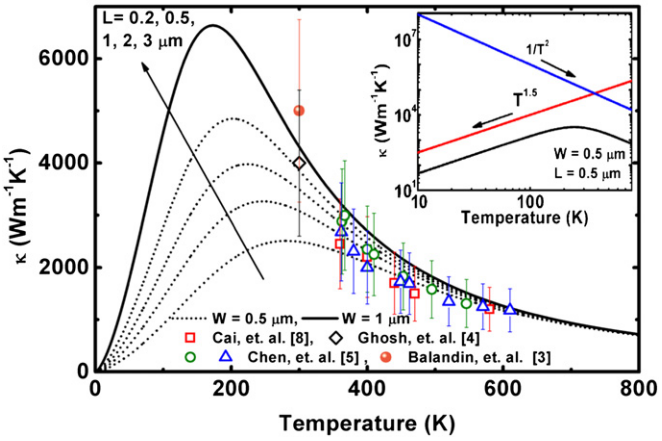

Figure 1. κ as a function of temperature for suspended SLG in the absence of isotopic scattering over a rectangular trench of various dimensions. The solid and dashed curves correspond to the present analytical model equation (16). The symbols represent the experimental data from [3–5] and [8]. The inset exhibits the log plot of the same.

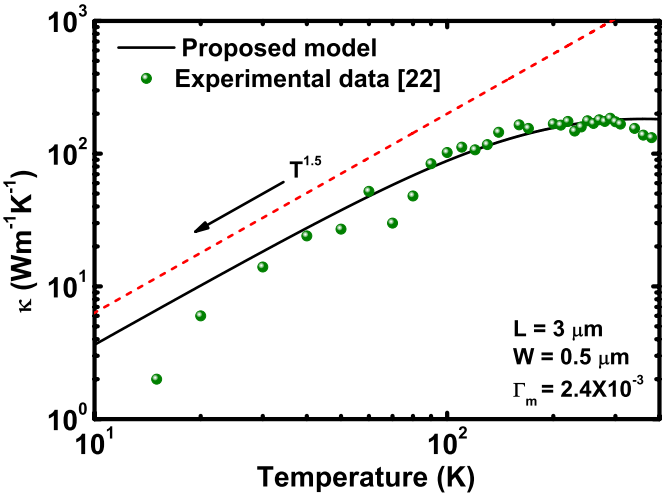

Figure 2. κ as a function of temperature for suspended SLG in the presence of isotopic scattering over a rectangular trench at the lower temperature regime. The solid curve corresponds to the present analytical model equation (16). The symbols represent the experimental data from [22]. The dashed line exhibits an eye guide to the reader exhibiting the nature of variation.

at high temperatures approaches unity. Thus, the total thermal conductivity can finally be modeled as

$$\kappa^{-1} = \kappa_{\text{low}}^{-1} + \kappa_{\text{high}}^{-1} \tag{16}$$

for both the aforementioned cases.

3. Model validation

Using equation (16), the variation of κ beyond room temperature has been exhibited in figure 1 for various flake dimensions. An excellent match has been exhibited using our analytical formulation in the absence of isotopes, i.e. using equation (14) for κ_{high}. The data points from Balandin *et al* [3] and Ghosh *et al* [4] at room temperature are at 5000 and 4000 W mK^{-1}; however, as the error bars in all graphene thermal experiments are as high as 30–40%, our modeling curves are within the accuracy of all the experiments with all different flake dimensions. The experimental data in [5, 8] were performed at the trench diameter which varies from approximately 3 to 10 μm, and were also well within our analytical curves. Furthermore, to correlate our analytical curves with the data of Balandin *et al* [3] and Ghosh *et al* [4], we have taken the trench length and width to be 3 and 1 μm to map their suspended SLG dimension experiments which are within 1–5 μm. The inset figure exhibits the effect of ZA flexural phonon on κ. When plotted as logarithmic axes, we see by using equations (11) and (13) that indeed the lower temperature region follows the $T^{1.5}$ law dominated by edge-roughness scattering, while beyond the room temperature, the trend follows a T^{-2} law due to the second-order three-phonon Umklapp process. It should be noted that in our model development, we have considered the second-order three-phonon Umklapp processes as suggested by Mingo and Broido which make κ to follow a T^{-2} behavior beyond room temperature, thus essentially removing the singularity by contributing a constant scattering rate at low frequencies [34].

Figure 2 exhibits the variation of κ with T in the low temperature zone. The symbols are taken from the experimental data of Xu *et al* between 15 and 380 K [22]. In this case, the suspended trench length is about 3 μm. We find that our theoretical model is in good agreement with the data in the specified region. The curve behavior mainly follows the $T^{3/2}$ law in the lower temperature region equation (11) (which dominates below room temperature) exhibiting the effect of ZA flexural phonons. At this point, it should be noted that Xu *et al* [22] mentioned about the trench's lateral dimensions to be about $W = 0.5$ μm; however, from the experimental data, it appears that κ is one order low if compared with the aforementioned references. This might be due to the two reasons that the authors provided [22], that there might be a substantially stronger effect because of the edge-roughness scattering and the effect of isotope impurity scattering due to about 1.1 % of ^{13}C in their experimental data, which we also feel could be the main reason why κ attains to a much lower value near the room temperature. It is due to these reasons, we use equation (13) into equation (16) with $\Gamma_m = 2.4 \times 10^{-3}$ to correlate with the experimental data.

Figure 3 exhibits the variation of κ as a function of temperature with increasing isotope impurity concentration. The symbols are taken from the recent experimental observation by Chen *et al* [15] where the SLG was suspended over a circular trench of about 2.8 μm diameter. Using equation (16) by considering equation (13), we have analytically demonstrated the variation of κ over the temperature range of 300–650 K. In this case, we use the flake dimensions to be $L = 2$ μm and $W = 3$ μm. A choice of this dimension is taken to justify the suspended area match, namely $\pi\ (2.8/2)^2\ \mu\text{m}^2 \sim 3 \times 2\ \mu\text{m}^2$. Exploiting these considerations, we find that there is an excellent match between the observed data and our analytical curves which are well within the experimental error range. Since the specific value of Γ_m is rather unspecified, we take $\Gamma_m = 3$, 6 and

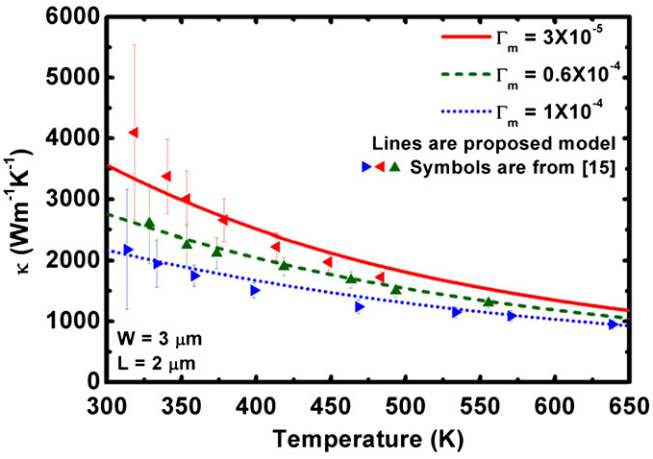

Figure 3. κ as a function of temperature for suspended SLG in the presence of isotopic scattering over a rectangular trench at the higher temperature regime. The solid and dashed curves correspond to the present analytical model equation (16). The symbols represent the experimental data from [15].

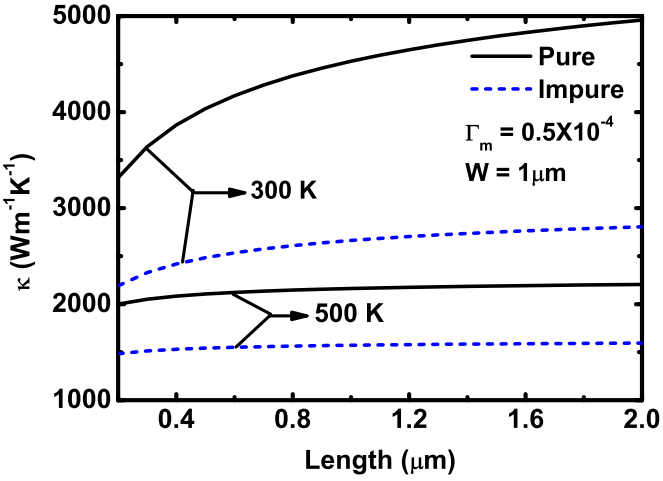

Figure 4. κ as a function of length for suspended SLG both in the presence and absence of isotopic scattering at 300 and 500 K.

10×10^{-5} to bring a close match between the experimental data set and our proposed model for 0.01%, 1.1% and 50% ^{13}C, respectively. It should be noted particularly that Chen *et al* [15] did not consider the effect of ZA flexural phonons on the determination of the thermal conductivity. Instead, they assumed that the phonon velocity does not modify in the presence of isotopes. However we feel that the treatment of ZA flexural phonons should be incorporated for the proper behavior of κ over the entire temperature range as the quadratic phonon dispersion relation signifies a higher phonon density of states [20] which effectively aids increasing the transport of heat in suspended SLGs. This is suggested from the fact that the phonon velocity is to be related to the phonon dispersion relation through a quadratic function (equation (1)). If however the phonon velocities are termed constant or say an average value between two extremes, there might appear an error in the determination of isotopically doped SLG thermal conductivity.

The variation of κ as a function of length has been demonstrated in figure 4 both for pure and impure SLGs at

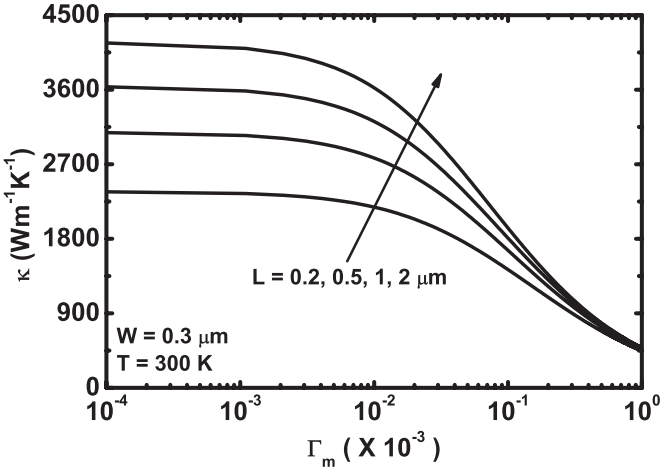

Figure 5. κ as a function of strength of the isotopic scattering for suspended SLG for varying length at room temperature.

300 and 500 K. It appears that κ increases more rapidly at 300 K rather than at 500 K for a width of 1 μm. Increasing the impurity to 5×10^{-5} cuts down κ to about one half of its value when intrinsic at 300 K and is almost constant at a value of about 2800 W m^{-1} K^{-1}. This effect has further been exhibited in figure 5 where κ is plotted against Γ_m at room temperature for a range of lengths. It appears that κ decreases with an increase in Γ_m and can reach as low as 450 W m^{-1} K^{-1} for $W = 0.3$ μm at $\Gamma_m = 10^{-3}$. As Γ_m decreases, κ tends to its respective intrinsic value. However as Γ_m increases, the phonons are strongly scattered more than the edge-roughness process; thus, κ tends to be independent of SLG length.

At this point, we wish to state that we have taken the Debye temperature of SLG flake to be 1000 K, a value widely taken for single walled carbon nanotube (SWCNT) [32]. Principally using the valance-force-field method, Nika *et al* [11] suggested that γ for the out-of-plane phonon mode should be very large which makes the contribution of the in-plane phonons surpass the out-of-plane phonons. It has further been suggested by Kong *et al* that γ for ZO modes is between -1.38 and -0.17, whereas for ZA modes, it is within -53 and -1.46 [40]. We thus take the ZA phonon mode Gruneisen parameter to be equal to -1.24, a value similar to that of SWCNT [41] and in between the LA mode (1.8) and TA mode (0.75) [2]. Using these values, we find that our proposed closed-form analytical model is in excellent match with the available experimental values. In addition, the geometric parameter F has been restricted to a value 2.5 for the figures 1, 3, 4 and 5 to standardize our theoretical model while $F = 0.08$ in figure 2 to present the interaction between the edge-roughness and heavy isotopic impurity scatterings. Finally, we wish to conclude this section by noting the fact that the dominance of the ZA flexural mode due to a higher phonon density of states makes κ follow a $T^{1.5}$ dependence instead of a T^2 dependence due to the in-plane LA and TA modes, respectively. This is the main reason behind neglecting the contribution of both the in-plane modes on κ as exhibited in equation (1).

4. Conclusions

The thermal conductivity of suspended SLG has been analytically presented using the exact quadratic behavior of ZA flexural phonons. Using this, we show that at lower temperature, κ exhibits a $T^{1.5}$ behavior due to the edge-roughness scattering, while beyond room temperature, it is the Umklapp scattering which dominates and makes κ follow a T^{-2} behavior. We find that these behaviors in our model are best explained through the upper limit of Debye cut-off frequency in the second-order three-phonon Umklapp scattering of the long phonon waves that actually remove the thermal conductivity singularity by contributing a constant scattering rate at low frequencies. The effect of isotopic scattering has also been included which lowers the value of κ significantly. Excellent experimental match has been found that validates our theoretical model over a wide range of temperatures.

References

[1] Sarkar D, Xu C, Li H and Banarjee K 2011 *IEEE Trans. Electron Devices* **58** 843
[2] Balandin A A 2011 *Nature Mater.* **10** 569
[3] Balandin A A, Ghosh S, Bao W, Calizo I, Teweldebrhan D, Miao F and Lau C N 2008 *Nano Lett.* **8** 902
[4] Ghosh S, Calizo I, Teweldebrhan D, Pokatilov E P, Nika D L, Balandin A A, Bao W, Miao F and Lau C N 2008 *Appl. Phys. Lett.* **92** 151911
[5] Chen S *et al* 2011 *ACS Nano* **5** 321
[6] Lee J U, Yoon D, Kim H, Lee S W and Cheong H 2011 *Phys. Rev.* B **83** 081419
[7] Pettes M T, Jo I, Yao Z and Shi L 2011 *Nano Lett.* **11** 1195
[8] Cai W, Moore A L, Zhu Y, Lee X, Chen S, Shi L and Ruoff R S 2010 *Nano Lett.* **10** 1645
[9] Jang W, Chen Z, Bao W, Lau C N and Dames C 2010 *Nano Lett.* **10** 3909
[10] Liao A D, Wu J Z, Wang X, Tahy K, Jena D, Dai H and Pop E 2011 *Phys. Rev. Lett.* **106** 256801
[11] Nika D L, Pokatilov E P, Askerov A S and Balandin A A 2009 *Phys. Rev.* B **79** 155413
[12] Nika D L and Balandin A A 2012 *J. Phys.: Condens. Matter* **24** 233203
[13] Ghosh S, Bao W, Nika D L, Subrina S, Pokatilov E P, Lau C N and Balandin A A 2010 *Nature Mater.* **9** 555
[14] Nika D L, Ghosh S, Pokatilov E P and Balandin A A 2009 *Appl. Phys. Lett.* **94** 203103
[15] Chen S, Wu Q, Mishra C, Kang J, Zhang H, Cho K, Cai W, Balandin A A and Ruoff R S 2012 *Nature Mater.* **11** 203
[16] Aksamija Z and Knezevic I 2011 *Appl. Phys. Lett.* **98** 141919
[17] Saito K, Nakumara J and Natori A 2007 *Phys. Rev.* B **76** 115409
[18] Sevincli H and Cuniberti G 2010 *Phys. Rev.* B **81** 113401
[19] Mariani E and von Oppen F 2008 *Phys. Rev. Lett.* **100** 076801
[20] Lindsay L, Broido D A and Mingo N 2010 *Phys. Rev.* B **82** 115427
[21] Lindsay L, Broido D A and Mingo N 2011 *Phys. Rev.* B **83** 235428
[22] Xu X *et al* 2010 arXiv:1012.2937
[23] Munoz E, Lu J and Yakobson B I 2010 *Nano Lett.* **10** 1652
[24] Xu X *et al* 2012 *PHONONS 2012: 14th Int. Conf. on Phonon Scattering in Condensed Matter (Ann Arbor, MI, 8–13 July 2012)*
[25] Ong Z-Y and Pop E 2011 *Phys. Rev.* B **84** 075471
[26] International roadmap to semiconductors http://www.itrs.net/Links/2009ITRS/2009Chapters_2009Tables/2009_Interconnect.pdf
[27] Li X, Maute K, Dunn M L and Yang R 2010 *Phys. Rev.* B **81** 245318
[28] Sun K, Stroscio M A and Dutta M 2009 *J. Appl. Phys.* **105** 074316
[29] Landau L D and Lifshitz E M 1986 *Theory of Elasticity* (New York: Pergamon)
[30] Castro E V, Ochoaa H, Katsnelson M I, Gorbachev R V, Elias D C, Novoselov K S, Geim A K and Guinea F 2010 *Phys. Rev. Lett.* **105** 266601
[31] Ochoaa H, Castro E V, Katsnelsonc M I and Guinea F 2012 *Physica* E **44** 963
[32] Hone J, Batlogg B, Benes Z, Johnson A T and Fisher J E 2000 *Science* **289** 1730
[33] Holland M G 1963 *Phys. Rev.* **132** 2461
[34] Mingo N and Broido D A 2005 *Nano Lett.* **5** 1221
[35] Ziman M 1960 *Electrons and Phonons* (Oxford: Oxford University Press)
[36] Nika D L, Askerov A S and Balandin A A 2012 *Nano Lett.* **12** 3238
[37] Nika D L, Pokatilov E P and Balandin A A 2011 *Phys. Status Solidi* b **248** 2609
[38] Liu W and Balandin A A 2005 *J. Appl. Phys.* **97** 073710
[39] Singh D, Murthy J Y and Fisher T S 2011 *J. Appl. Phys.* **110** 044317
[40] Kong B D, Paul S, Nardelli B and Kim K W 2009 arXiv:0902.0642v1
[41] Reich S, Jantoljak H and Thomsen C 2000 *Phys. Rev.* B **61** R13389